Journal of Pharmaceutical and Biomedical Analysis 51 (2010) 1037–1046

Contents lists available at ScienceDirect

Journal of Pharmaceutical and Biomedical Analysis

journal homepage: www.elsevier.com/locate/jpba

Identification and characterization of degradation products of irbesartan using LC–MS/TOF, MS^n, on-line H/D exchange and LC–NMR

Ravi P. Shah, Archana Sahu, Saranjit Singh*

Department of Pharmaceutical Analysis, National Institute of Pharmaceutical Education and Research (NIPER), Sector 67, S.A.S. Nagar, 160062, Punjab, India

ARTICLE INFO

Article history:
Received 12 August 2009
Received in revised form 5 November 2009
Accepted 6 November 2009
Available online 13 November 2009

Keywords:
Irbesartan
Degradation products
LC–MS/TOF
On-line H/D exchange
LC–NMR

ABSTRACT

Irbesartan was subjected to hydrolytic, oxidative, photolytic and thermal stress, according to ICH guideline Q1A (R2). The drug showed degradation only in acidic, basic and photoacidic conditions, while it was stable to other stress conditions. A total of three degradation products were formed, which were separated on a C-8 column employing a gradient HPLC method. Initially, a complete mass fragmentation pathway of the drug was established with the help of MS/TOF, MS^n and H/D exchange studies. Subsequently, the degradation products were subjected to LC–MS/TOF and on-line H/D exchange mass studies to obtain their accurate mass, fragment pattern and number of labile hydrogens. The MS results helped to assign tentative structures to degradation products, which were verified through ^1H and 2D COSY LC–NMR experiments. The products were identified as (2′-(1H-tetrazol-5-yl)biphenyl-4-yl)methanamine, 1-(1-((2′-(1H-tetrazol-5-yl)biphenyl-4-yl)methylamino)pentylideneamino)cyclopentane carboxylic acid and 2-butyl-3-(tetrazolo[1,5-f]phenanthridin-6-ylmethyl)-1,3-diazaspiro[4.4]non-1-en-4-one. The structures were justified by mechanisms of their formation.

1. Introduction

It is a well known fact that drugs undergo physicochemical degradation upon storage. Thus, stability testing of a drug under various temperature and humidity conditions is indispensable during the drug development process. In addition, stability testing guidelines issued by International Conference on Harmonization (ICH) and other international agencies [1–4] require the reporting, identification and characterization of degradation products (DPs). But, as DPs generated during storage may be in very low levels (~0.1–0.5%, w/w), stress studies are suggested to generate them in higher amounts [5]. Still sometimes it is very difficult to isolate these species from the stressed mixture due to their low amounts and subject them to spectral analyses for structural information. Therefore, hyphenated techniques like LC–MS and LC–NMR are currently extensively used for this purpose [6–11].

Irbesartan is an angiotensin II receptor antagonist used in the treatment of hypertension [12,13]. Although it has been in the market for over 10 years, only scant information exists on stability and degradation behaviour of the drug. An investigation was carried out by Mbah [14] on the kinetics of breakdown of irbesartan in aqueous solutions at elevated temperatures. The reaction was found to follow first-order kinetics. The decomposition was shown to be hydroxide ion catalysed and the effects of ionic strength and buffer concentrations on such rate studies were discussed. In addition, Hillaert et al. mentioned of instability of irbesartan in basic solution as a hurdle faced during chromatographic method development [15]. The formation of formaldehyde–irbesartan adduct on storage of film coated tablet is also reported [16]. As there is no comprehensive report on degradation chemistry of the drug, therefore, the endeavour of the present study was to: (i) carry out the stress studies on irbesartan under the ICH prescribed conditions; (ii) separate the degradation products by HPLC; and (iii) characterize all the degradation products with the help of LC–MS/TOF, on-line H/D exchange and LC–NMR investigations.

2. Experimental

2.1. Drug and reagents

Pure irbesartan was obtained as gratis sample from Ranbaxy Research Laboratories (Gurgaon, India) and it was used without further modification. Analytical reagent (AR) grade sodium hydroxide (NaOH) was purchased from Ranbaxy Laboratories (S.A.S. Nagar, India), hydrochloric acid (HCl) from LOBA Chemie Pvt. Ltd. (Mumbai, India) and hydrogen peroxide (H_2O_2) from s.d. fine-chem Ltd. (Boisar, India). Buffer salts and all other chemicals of AR grade were bought from local suppliers. HPLC grade acetonitrile (ACN) and methanol (MeOH) were procured from J.T. Baker (Phillipsburg,

* Corresponding author. Tel.: +91 172 2214682; fax: +91 172 2214692.
E-mail address: ssingh@niper.ac.in (S. Singh).

0731-7085/$ – see front matter © 2009 Elsevier B.V. All rights reserved.
doi:10.1016/j.jpba.2009.11.008

Table 1
Stress conditions for optimum degradation.

Stress condition	Concentration of stressor	Exposure condition	Duration
Hydrolysis			
Acid	1N HCl	80 °C	24 h
Neutral	H_2O		48 h
Base	2N NaOH		48 h
Oxidation	30% H_2O_2	RT	2 d
Photolysis	8500 lx fluorescent and 0.05 W/m^2 UV light		
Acid	0.01N HCl	40 °C/75% RH	4 d
Neutral	H_2O		13 d
Base	0.01N NaOH		13 d
Solid	–		13 d
Thermal	–	50 °C	21 d

NJ, USA). Deuterated methanol (CD_3OD) and water (D_2O) of 99.6% purity were obtained from Aldrich (California, Missouri, USA). ES Tuning Mix solution (Agilent Technologies, USA) was used as the MS/TOF calibrant. Water for HPLC studies was obtained from ultrapure water purification unit (Elga, Wycombe, England).

2.2. Apparatus and equipment

Precision water baths equipped with MV controller (Julabo, Seelbach, Germany) were used for solution degradation studies. A Dri-Bath (Thermolyne, IA, USA) was used for solid state thermal stress study. Accelerated stability studies were carried out in humidity (KBF720, WTC Binder, Tuttlingen, Germany) and photostability (KBWF 240, WTC Binder, Tuttlingen, Germany) chambers, both set at 40 ± 1 °C/75 ± 3% RH. The photostability chamber was equipped with an illumination bank on inside top, consisting of a combination of two UV (OSRAM L18 W/73) and four white fluorescent (PHILIPS TRULITE 18W/86) lamps, in accordance with Option 2 of the ICH guideline Q1B [17]. Both fluorescent and UV lamps were put on simultaneously. The samples were placed at a distance of 0.23 m from the light bank. A lux meter (model ELM 201, Escorp, New Delhi, India) and a UV radiometer (model 206, PRC Krochmann GmbH, Berlin, Germany) were used to measure visible illumination and UV energy, respectively.

A pH/Ion analyzer (MA 235, Mettler Toledo, Schwerzenbach, Switzerland) was used to check and adjust the pH of buffer solutions. Other small equipments were sonicator (3210, Branson Ultrasonics Corporation, Danbury, CT, USA), precision analytical balance (AG 135, Mettler Toledo, Schwerzenbach, Switzerland) and auto pipettes (Eppendorf, Hamburg, Germany).

The LC-UV system consisted of basic modules and was equipped with a photo-diode array detector (all from Shimadzu, Kyoto, Japan). The system was controlled by Class-VP software (version 6.14 SP1). On-line H/D exchange and multi-stage mass studies (MS^n) were carried out on a LC–MS ion trap instrument (Thermo, San Jose, USA) wherein the LC system (Accela) was connected with MS (LTQ XL MS 2.5.0) via an ESI source and controlled by Xcalibur (version 2.0.7 SP1). LC–MS/TOF studies were carried out on a system in which HPLC (1100, Agilent Technologies, Waldbronn, Germany) was hyphenated to MicrOTOF-Q spectrometer (Bruker Daltonik, Bremen, Germany). It was controlled using Hyphenation Star (version 3.1) and MicrOTOF Control (version 2.0) software. In all the studies, separations were achieved on a Discovery C-8 column (250 mm × 4.6 mm i.d., particle size 5 μm) procured from Supelco (Bellefonate, PA, USA). LC–NMR measurements were taken using JNM-ECA 500 MHz spectrometer (JEOL, Japan) coupled to Prominence HPLC system (Shimadzu, Kyoto, Japan), controlled by Delta (Version 4.3) and LC-NMR Dio (Version 2.0) software, respectively.

2.3. Stress studies

Stress studies were carried out under ICH recommended conditions of hydrolysis, photolysis, oxidation and dry heat. The optimized stressed conditions are enlisted in Table 1.

The stressors, choice of their concentration and preparation of samples were based on our previous publication [5]. As the drug was insoluble in water, it was dissolved in a mixture of ACN and water in a ratio of 50:50 (v/v). The concentration of the drug in stock

Table 2
Parameters for MS/TOF studies in ESI positive mode.

Mode		Parameters for M+H	Parameters for fragment study
Source	End plate offset (V)	−500	−500
	Capillary (V)	−4500	−4500
	Nebuliser (Bar)	1.2	1.2
	Dry gas (L/min)	6.0	6.0
	Dry temperature (C)	200	200
Transfer	Funnel 1 RF (Vpp)	200	200
	Funnel 2 RF (Vpp)	250	220
	ISCID energy (eV)	0.0	4.0
	Hexapole RF (Vpp)	300	240
Quadrupole	Ion energy	4.0	4.0
	Low mass (m/z)	300	200
Collision cell	Collision energy (eV/z)	7.0	35
	Transfer time (μs)	48	35
	Collision RF (Vpp)	310	240
	Pre-pulse storage (μs)	8.0	8.0
Detector	Source (V)	−1200	−1200

solution was 2 mg/ml. It was diluted 50:50 (v/v) with the stressor (e.g., HCl, NaOH, water). After subjecting to stress, samples were withdrawn at suitable time intervals and diluted four times with ACN and water (50:50, v/v) before injecting into HPLC.

2.4. HPLC method development and optimization

The separation of drug and its DPs was initially tried using different proportions of MeOH (A) and potassium dihydrogen phosphate buffer (0.01 M) (B) and also by varying pH of buffer with phosphoric acid. The acceptable resolution was achieved by using buffer of pH 3.0 along with the organic modifier in a gradient mode (T_{min}/A:B; T_0/15:85; T_6/70:30; T_{15}/70:30; T_{20}/15:85). The detection wavelength and flow rate were 250 nm and 1.0 ml/min, respectively. For LC–MS studies, the buffer component B was replaced by 0.01 M ammonium acetate solution of the same pH.

However, two separate isocratic HPLC methods were developed for LC–NMR investigations, both involving phosphate buffer (pH 3.0) as component B of the mobile phase and flow rate of 0.5 ml/min. In the first method, the mobile phase consisted of A:B in a ratio of 40:60, while the ratio was 60:40 for the second method. The former was used for collection of NMR data of DP-I, while the latter was employed for drug, DP-II and DP-III.

2.5. MS/TOF, MS^n and H/D exchange studies on drug

The elucidation of mass fragmentation pattern of the drug was achieved with the help of MS/TOF, MS^n and H/D exchange data. MS/TOF studies were performed in ESI positive mode, and various parameters were suitably optimized in order to get clear information regarding the molecular ion peak of the drug. The mass parameters were further modified to get complete fragmentation of the drug. The optimized parameters are listed in Table 2. In the subsequent step, the information on the origin of each individual fragment was obtained from MS^n studies. Fragmentation of various precursor ions was achieved at different normalized collision energies. The structure of each fragment was further verified with the help of H/D exchange studies, which were carried out by injecting drug solution in D_2O and CD_3OD (50:50%, v/v).

2.6. LC–MS/TOF and on-line H/D exchange studies on degradation products

The stressed samples were subjected to LC–MS/TOF analyses using the optimized MS/TOF parameters listed in Table 2. For internal calibration, the ES Tuning Mix solution was injected through a diverter in a specific segment near the peak of interest. The on-line H/D exchange mass studies were carried out through injection of D_2O via an additional channel of the MS^n system, just before the peak of interest started eluting from the column. The flow of D_2O was continued until the peak was completely eluted.

2.7. LC–NMR studies on drug and degradation products

For LC–NMR studies, all the stressed samples were first subjected to LC using the developed gradient methods, as discussed in Section 2.4. All the resolved peaks (drug and DPs) were collected in the fraction loop using terminal cube and sent to inverse 3 mm flow probe equipped with ^1H $\{^{13}C\}$ channels with pulsed-field gradient along *z*-axis. The active sample volume of the probe was approximately 60 μl and the transfer time from the UV cell to the active volume was 45 s at a flow rate of 0.5 ml/min. One-dimensional ^1H spectra were recorded using the WET pulse sequences, with attenuated power at 44 [dB] for solvent suppression of HOD signal, which gave digital resolution of 0.76, 0.57, 0.57, and 0.76 Hz per point for drug, DP-I, DP-II and DP-III, respectively. Spectra were acquired

Table 3
Interpretation of MS/TOF and MS^n data of fragments of the drug.

Peak no.	MS/TOF data (amu)	Best possible molecular formulae	Exact mass of most probable structure (amu)	Error in mmu	RDB	Possible parent fragment	Difference from parent ion (amu)	Possible molecular formulae for Loss		H/D exchange data (amu)		No. of labile hydrogens	
								L1	L2			$[M+H]^+$	M^+
M+H	429.2504	$C_{25}H_{29}N_6O$	429.2397	10.6	14.5	–				431		2	1
a	401.2391	$C_{25}H_{29}N_4O$	401.2336	5.5	13.5	M+H	28.0113	CH_2N	N_2	403		2	1
b	386.2262	$C_{25}H_{28}N_3O$	386.2227	3.5	13.5	a	15.0127	NH	CH_3	387		1	0
c	235.0998	$C_{14}H_{11}N_4$	235.0978	1.9	11.5	M+H	194.1489	$C_{11}H_{18}N_2O$	$C_{12}H_{20}NO$	236		1	0
d	207.0975	$C_{14}H_{11}N_2$	207.0917	5.8	10.5	a, c	194.1416, 28.0016	$C_{11}H_{18}N_2O$ N_2	$C_9H_{16}N_5$ CO	208		1	0
e	195.1519	$C_{11}H_{19}N_2O$	195.1492	2.7	3.5	M+H, a	234.0961 206.0848	$C_{14}H_{10}N_4$ $C_{14}H_{10}N_2$	$C_{15}H_{10}N_2O$ $C_8H_{10}N_6O$	197		2	1
f	192.0780	$C_{14}H_{10}N$	192.0808	2.7	10.5	b, d	15.0195, 194.146	NH $C_{11}H_{18}N_2O$	CH_3 $C_9H_{16}N_5$	192		0	0
g	180.0840	$C_{13}H_{10}N$	180.0808	3.2	9.5	b	206.1399	$C_{12}H_{18}N_2O$	$C_{10}H_{16}N_5$	181		1	0
h	178.0705	$C_{13}H_8N$	178.0651	5.3	10.5	f	14.0074	N	CH_2	178		0	0

RDB: ring plus double bonds; a–h: peak numbers shown in Fig. 2.

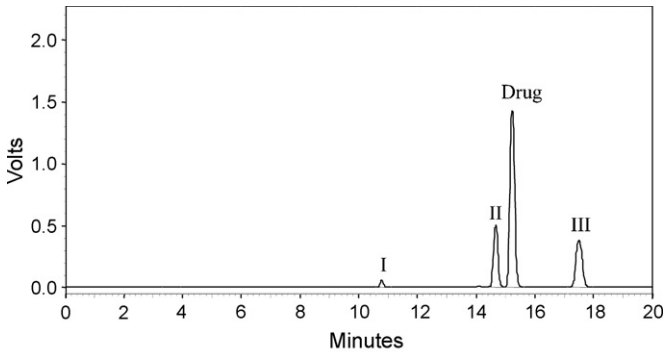

Peaks	I	II	III
Stress conditions	A	B	PA

Fig. 1. Chromatogram showing separation of degradation products (I–III) and drug in the mixture of stressed samples. *Key*: I–III: degradation products; A: acid; B: base; PA: photoacid.

with 15 kHz spectral width and 16 K data points. Depending on concentration of DPs, number of scans ranging between 512–2096 were accumulated to obtain an appropriate signal-to-noise ratio. The chemical shifts were referenced to the methyl signal of the residual CH_3CN at 1.93 ppm.

A 2D Correlation spectroscopy (COSY) spectrum of drug and DPs was acquired using WET pulse sequences for solvent suppression. A total of 96 scans were collected for each of the 256 iterations in the F_1 dimension, using a spectral width of ~10 kHz in both dimensions, yielding 1280 data points with digital resolution of 7.33 Hz per point.

3. Results and discussion

3.1. Degradation behaviour

The drug degraded into DP-I, DP-II and DP-III under acid, base and photoacid conditions, respectively. The respective extent of degradation was 4.5%, 51.4% and 48.7% under the three conditions. The chromatogram of the mixture of degraded samples is shown in Fig. 1. The drug was stable under all other stress conditions, including heating in water, oxidation, on exposure of aqueous and base solutions to light, photoexposure of solid drug, and dry heating at 80 °C.

Table 4
MS^n fragmentation of the drug.

MS^n	Precursor ion	Product ions
MS^2	429	401, 386, 235, 207, 195
MS^3	401	386, 207, 195
	235	207, 192, 178
MS^4	386	192, 180
	207	192, 178
MS^5	192	178

3.2. Mass fragmentation behaviour of the drug

Fig. 2 shows the line spectra of the drug obtained from MS/TOF studies. In total, eight fragments were formed from the drug (labelled 'a–h'). The most probable molecular formula for each fragment, calculated from experimental mass values with the help of Elemental Composition Calculator, is shown in Table 3. The table also includes H/D exchange data and errors in mmu. The data from MS^n studies (Table 4) were helpful to establish origin of each fragment. These were also useful in the calculation of accurate *m*/*z* values for the losses and their probable molecular formulae, which are included in Table 3.

The molecular ion peak of *m*/*z* 429 fragmented in MS^2 step into ions of *m*/*z* 401, 386, 235, 207 and 195 (Table 4). A critical inspection of the MS^2 spectrum indicated the presence of a pair of complementary fragment ions of *m*/*z* 235 and 195, which added to 430 Da and this corresponded to M+2H. Similarly, the fragment of *m*/*z* 401, on addition of 28 Da (neutral loss of N_2), was congruent to M+H. With these observations, it became apparent that the product ion spectrum could be dissected into two principal pathways, one leading to an ion of *m*/*z* 401 formed from charged tetrazole moiety, and fragments of *m*/*z* 235 and 195 resulting from charged 1,3-diazaspiro[4,4]non-1-en-4-one moiety. Thus it was possible to lay down the mass fragmentation profile of the drug, which is depicted in Fig. 3.

3.3. Mass studies on degradation products

The degradation products were subjected to MS/TOF studies in ESI positive mode to determine their molecular ion peaks and to establish their fragment profile. The instrument parameters were the same, as shown in Table 2. The accurate *m*/*z*

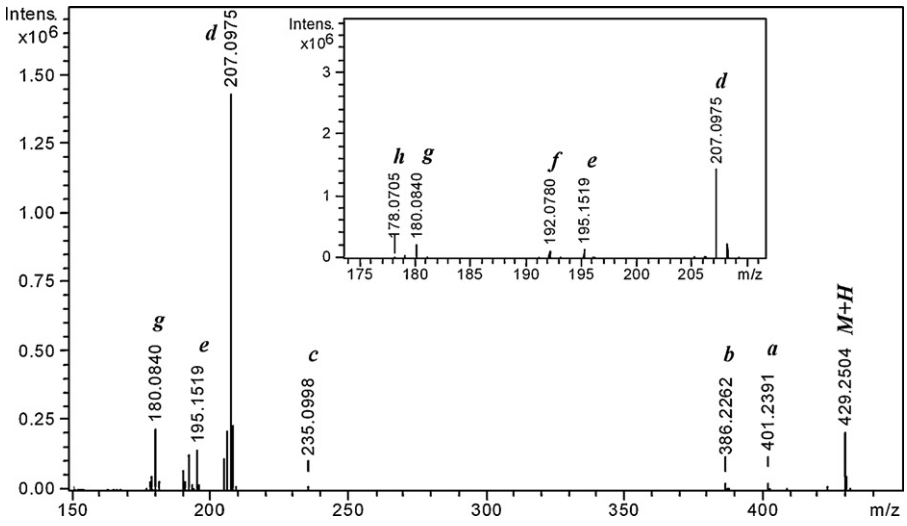

Fig. 2. Line spectrum of the drug obtained in an MS/TOF study.

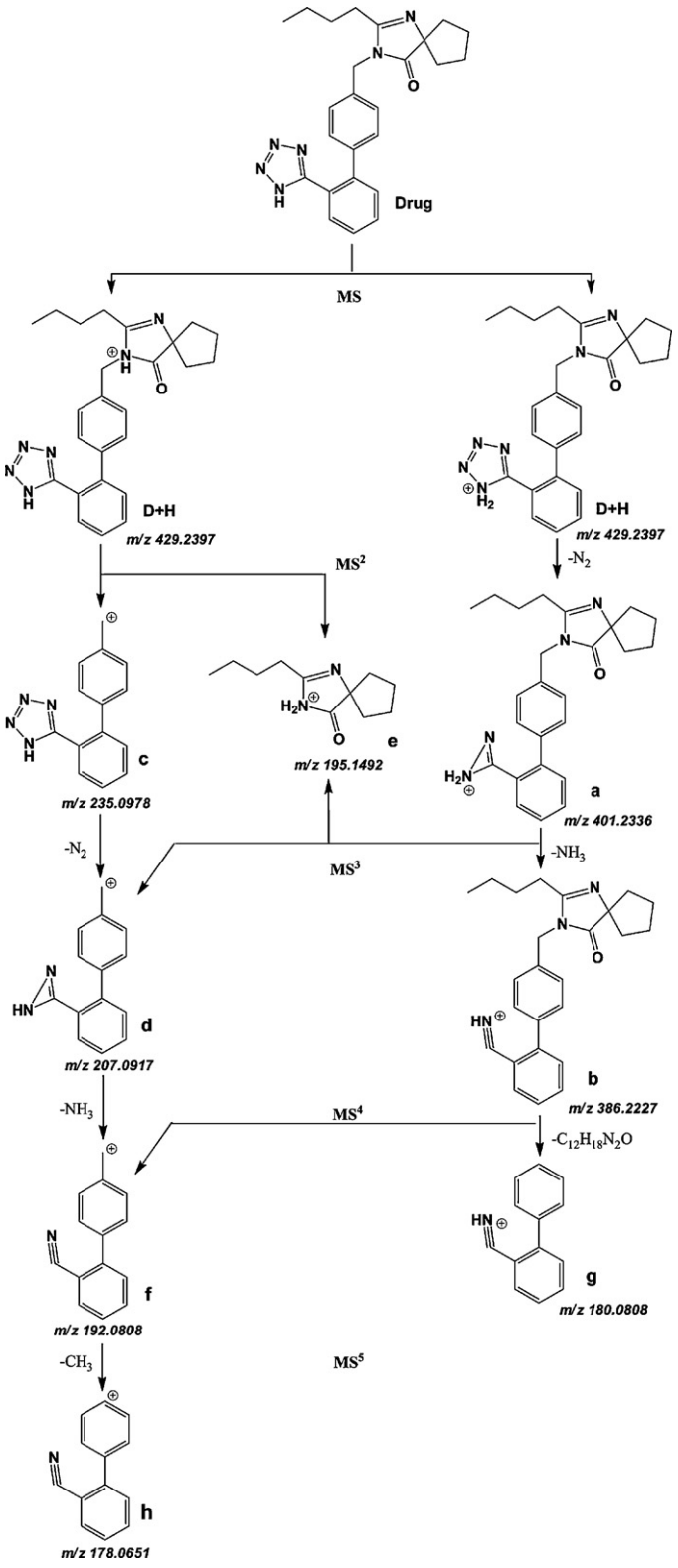

Fig. 3. Fragmentation pathway of the drug along with the exact masses of the fragments.

Table 5
MS/TOF and on-line H/D exchange data of DPs (I–III) along with their possible molecular formulae and major fragments.

DPs	MS/TOF values for M+H (amu)	Nitrogen rule	Probable molecular formulae (exact masses in amu; error in mmu; RDB)			Fragments of ESI positive mode in amu (molecular formula; error in mmu)	*m/z* after H/D exchange in ESI positive mode (amu)	No. of labile H in the structure
			P1	P2	P3			
I	252.1276	Odd	$C_{16}H_{16}N_2O^+$ (252.1257; 1.8; 10.0)	$C_{14}H_{14}N_5^+$ (252.1243; 3.2; 10.5)	$C_{15}H_{16}N_4^+$ (251.1369; −9.3; 10.0)	235.1026 ($C_{14}H_{11}N_4^+$; 4.7), 224.1129 ($C_{14}H_{14}N_3^+$; −5.3), 207.0969 ($C_{14}H_{11}N_2^+$; 5.2), 192.0750 ($C_{14}H_{10}N^+$; −5.7), 180.0869 ($C_{13}H_{10}N^+$; 6.1), 178.0798 ($C_{13}H_8N^+$; 14.6)	256	3
II	447.2523	Even	$C_{25}H_{31}N_6O_2^+$ (447.2503; 2.0; 13.5)	$C_{26}H_{33}N_5O_2^+$ (447.2628; −10.5; 13.0)	–	252.1274 ($C_{14}H_{14}N_5^+$; 3.0), 235.1026 ($C_{14}H_{11}N_4^+$; 4.7), 207.0967 ($C_{14}H_{11}N_2^+$; 5.0), 196.1385 ($C_{11}H_{18}NO_2^+$; 5.2), 192.0747 ($C_{14}H_{10}N^+$; −6.0), 180.0865 ($C_{13}H_{10}N^+$; 5.7), 178.0817 ($C_{13}H_8N^+$; 16.5), 168.1443 ($C_{11}H_{18}NO^+$; 6.0)	451	3
III	427.2300	Even	$C_{27}H_{29}N_3O_2^+$ (427.2254; 4.5; 15.0)	$C_{25}H_{27}N_6O^+$ (427.2240; 5.9; 15.5)	–	399.2240 ($C_{25}H_{27}N_4O^+$; 6.0), 233.0861 ($C_{14}H_9N_4^+$; 3.9), 205.0824 ($C_{14}H_9N_2O^+$; 6.3), 195.1544 ($C_{11}H_{19}N_2O^+$; 5.2), 178.0708 ($C_{13}H_8N^+$; 5.6)	428	0

Table 6
^{1}H chemical shift assignments for irbesartan and its degradation products DP-I–III.

Position	δ_H/ppm (multiplicity)			
	Drug	DP-I	DP-II	DP-III
6	1.97 (m)	–	1.78 (m)	2.10 (m)
7	1.85 (m)	–	1.59 (m)	[a]
8	1.85 (m)	–	1.59 (m)	[a]
9	1.97 (m)	–	1.78 (m)	2.10 (m)
10	[a]	4.03 (s)	4.23 (s)	5.14 (s)
12	7.02 (d)	7.08 (d)	6.92 (d)	7.65 (d)
13	7.07 (d)	7.28 (d)	7.11 (d)	8.67 (d)
15	7.05 (d)	7.27 (d)	7.11 (d)	–
16	7.00 (d)	7.07 (d)	6.92 (d)	8.39 (s)
19	7.53 (d)	7.61 (d)	7.57 (d)	8.54 (d)
20	7.48 (t)	7.50 (t)	7.47 (t)	7.82 (t)
21	7.58 (t)	7.60 (t)	7.54 (t)	7.93 (t)
22	7.42 (d)	7.48 (d)	7.42 (d)	8.61 (d)
28	[a]	–	2.06 (m)	[a]
29	1.35 (m)	–	1.37 (m)	1.43 (m)
30	1.18 (m)	–	1.14 (m)	1.19 (m)
31	0.70 (t)	–	0.73 (t)	0.59 (t)

[a] ^{1}H peaks were not observed due to CH_3CN and HOD suppression at that region.

values for the molecular ion peaks as well as fragments of degradation products are given in Table 5. Using observed accurate *m*/*z*, the molecular formulae were generated with the help of Elemental Composition Calculator. The numbers of exchangeable hydrogens present in the structure of each DP, obtained with the help of on-line H/D exchange studies, are given in Table 5.

3.4. LC–NMR studies on drug and degradation products

The LC–^{1}H NMR data for the drug and DPs are listed in Table 6. The peaks corresponding to alkyl chain of the drug (at δ 0.5–3.0) were absent in DP-I, although these peaks were present in DP-II and DP-III. The peaks in the aromatic region between δ 7.0 and 9.0 of DP-III were different from the drug and other DPs. Two-dimensional COSY LC–NMR spectra revealed some important structural connectivities. When compared to the drug (Fig. 4), the correlation peaks for DP-III were diagnostic for the spin-systems belonging to the benzene ring (*C*11-*C*16; Fig. 5).

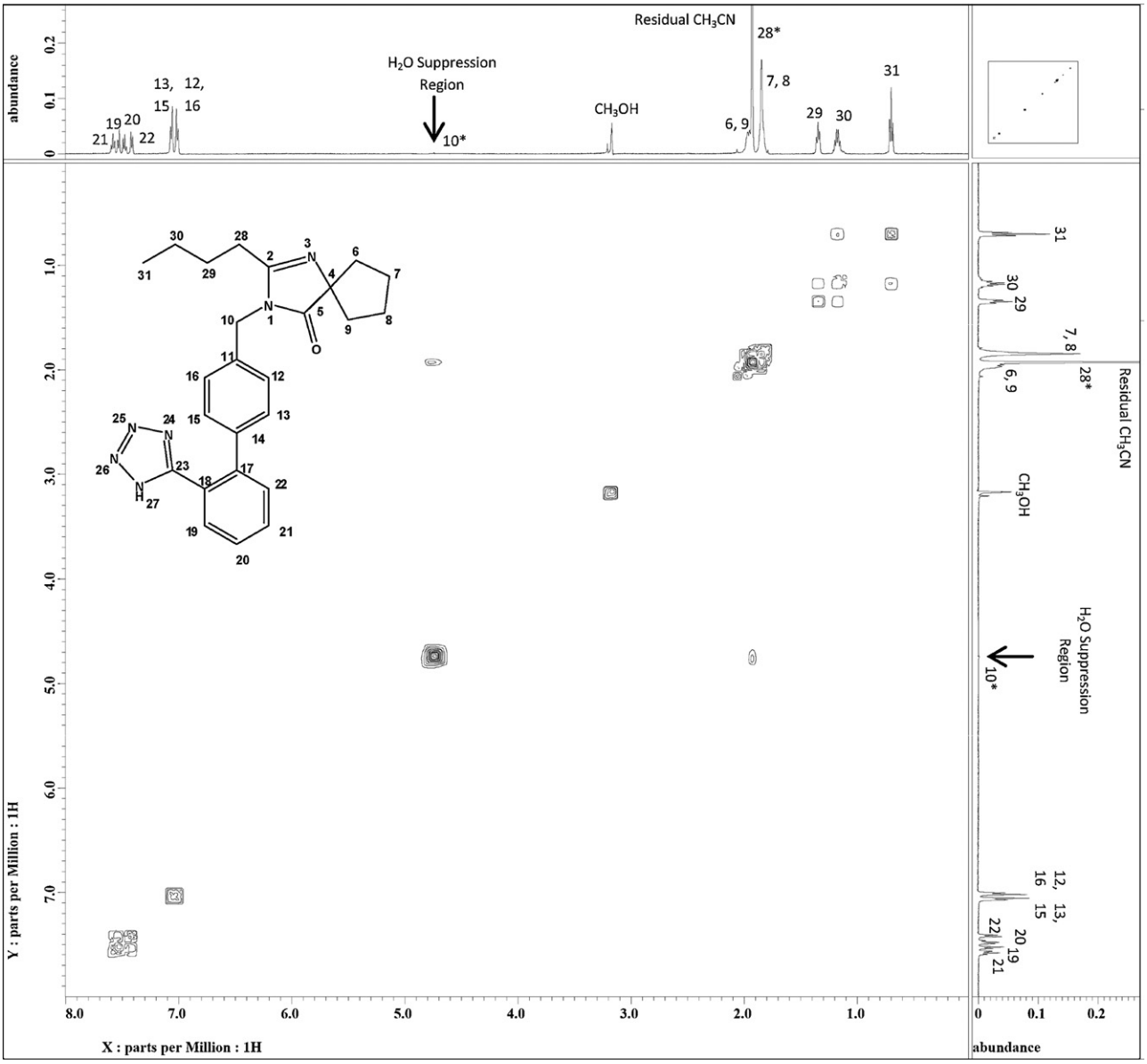

Fig. 4. 2D LC–COSY NMR spectrum of the drug. *Key*: *^{1}H peaks were not observed due to CH_3CN and HOD suppression at that region.

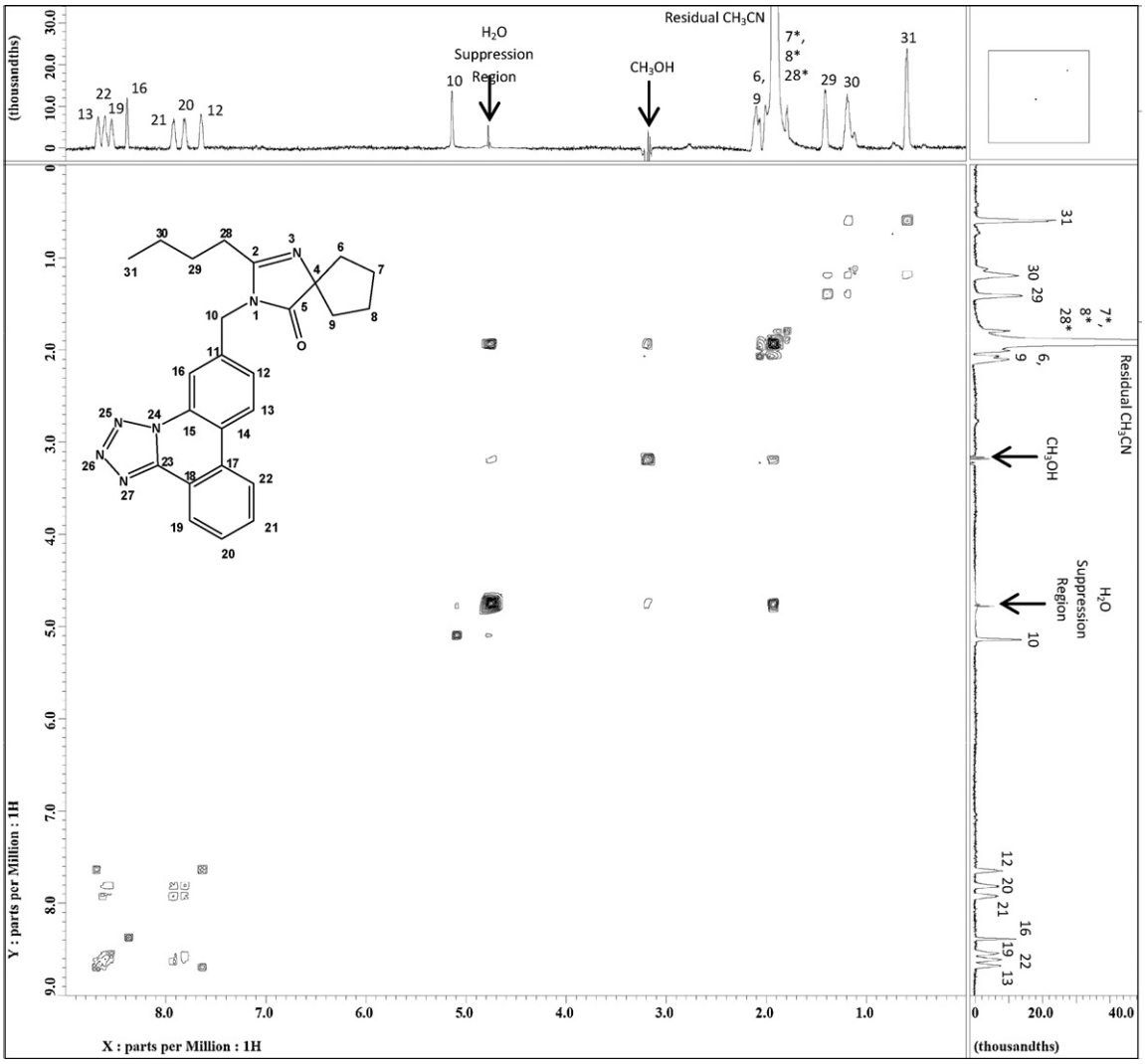

Fig. 5. 2D LC–COSY NMR spectrum of DP-III. *Key*: *[1]H peaks were not observed due to peak of CH_3CN at that region.

3.5. Characterization of degradation products

The structure elucidation of all the degradation products was achieved with the systematic amalgamation of HRMS, mass fragmentation, on-line H/D exchange and LC–NMR data.

3.5.1. DP-I

The experimental accurate *m*/*z* value of DP-I was 252.1276 Da, while nitrogen rule indicated the presence of an odd number of nitrogens in the structure. Of the three molecular formulae generated by Elemental Composition Calculator, only one had the said odd number, i.e., $C_{14}H_{14}N_5^+$, for which corresponding error between exact (252.1243 Da) and observed mass (252.1276 Da) was just 3.2 mmu. Further, the on-line H/D exchange study in positive ion mode resulted in molecular ion peak of *m*/*z* 256, indicating the presence of three labile hydrogens in the structure of DP-I. The same could be attributed to either three –NH groups or a combination of one each of –NH and $–NH_2$ groups. The presence of identical fragments of *m*/*z* of 235, 207, 192 and 178 of DP-I (Table 5) in parallel to those of the drug (Table 3 and Fig. 3) indicated that tetrazole ring attached to biphenyl was intact in the product. This meant involvement of –NH in the tetrazole ring, with $–NH_2$ moiety present as a free group. Accordingly, the structure and fragmentation pathway of DP-I was proposed, as shown in Fig. 6. Interestingly, this structure has also been reported as a photolytic degradation product of losartan, a drug congener of irbesartan [18].

The postulated structure was well supported by LC–NMR studies (Table 6). In ^{1}H NMR data of DP-I, all assignments corresponding to 2-butyl-1,3-diazaspiro[4,4]non-1-en-4-one moiety in the drug were absent between δ 0.0 and 2.0, showing removal of the alkyl portion. The downfield shift in DP-I at δ 4.03 suggested that $–CH_2$ group at position 10 was attached to 1° or 2° amine, unlike 3° amine in the drug. The absence of change in the aromatic region of both drug and DP-I was confirmed by comparison of 2D COSY LC–NMR spectra.

3.5.2. DP-II

Its accurate mass of *m*/*z* 447.2523 was ~18 Da higher than the drug. This clearly indicated addition of H_2O molecule to the drug. The nitrogen rule and Elemental Composition Calculator suggested $C_{25}H_{31}N_6O_2^+$ (theoretical mass 447.2503 Da) as the most probable molecular formula. The molecular ion peak of 451 obtained during on-line H/D exchange studies in ESI positive mode indicated the presence of three labile hydrogens, which again could be due to –NH, –OH and/or –COOH. But since DP-II was formed in basic

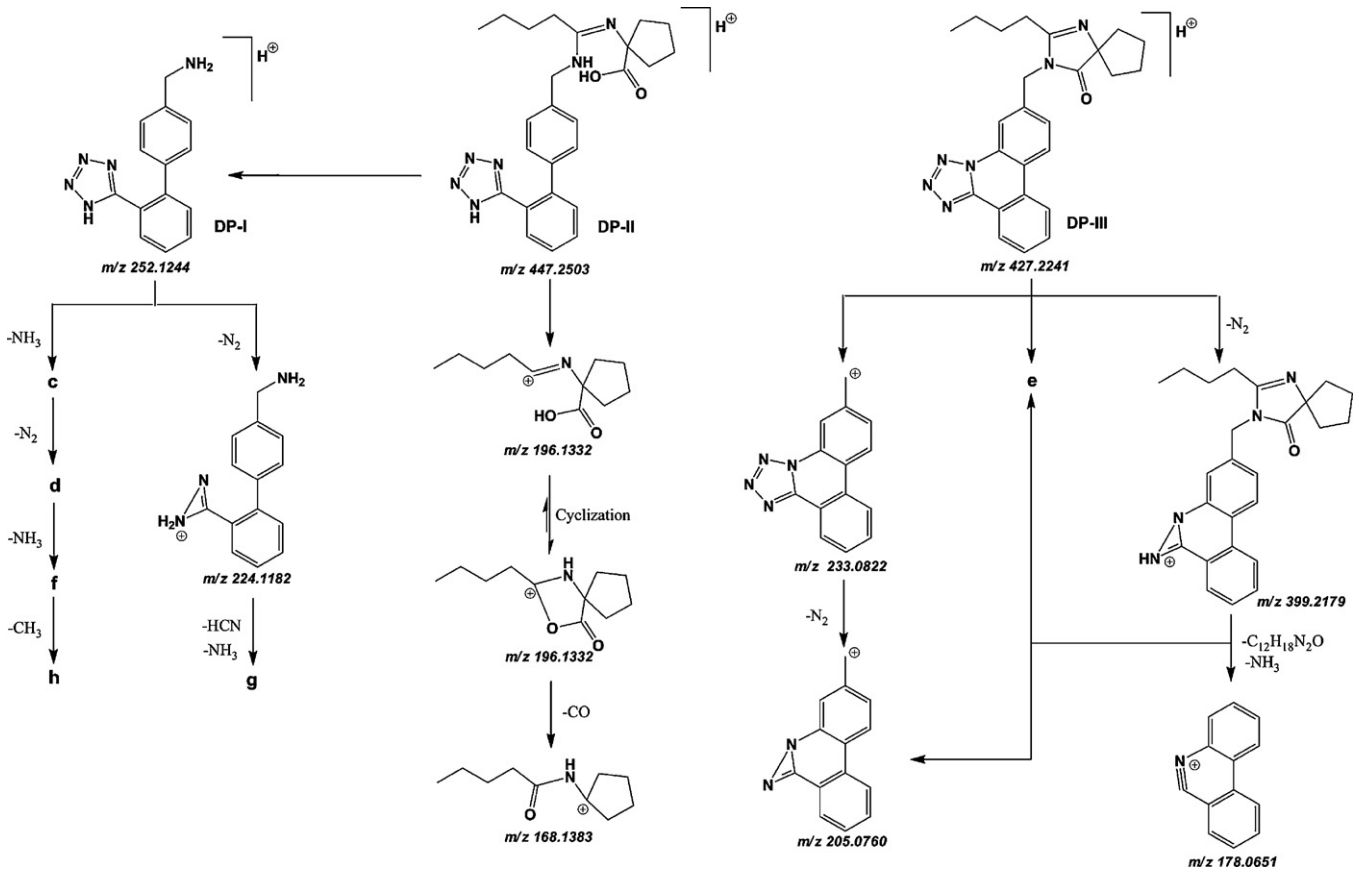

Fig. 6. Fragmentation pathway of the DPs (I–III) along with the exact masses of the fragments. *Key*: Structures of the fragments c, d and f–h were shown in Fig. 3.

condition, two of the labile hydrogens could be due to –COOH and $–NHR_2$ groups, formed upon hydrolysis of the $–CONR_2$ group of 1,3-diazaspiro[4,4]non-1-en-4-one moiety. The other labile hydrogen was attributed to –NH of tetrazole. Also, the fragments of *m*/*z* 235, 207, 192 and 178 of DP-II were identical to the drug (Table 5 and Table 3), which indicated the presence of tetrazole ring attached to biphenyl. Interestingly, DP-II had a typical fragment of *m*/*z* 196, with one mass unit higher than the drug fragment of *m*/*z* 195 (Fig. 3). This too indicated that DP-II was structurally different from the drug in the region of 1,3-diazaspiro[4,4]non-1-en-4-one. This fragment of *m*/*z* 196 was formed by the removal of *m*/*z* 252 ($C_{14}H_{14}N_5^+$) from DP-II, which further fragmented into *m*/*z* 168 after the loss of CO, as shown in Fig. 6. All other fragments were identical to DP-I.

Even the LC–^{1}H NMR data for DP-II (Table 6) showed similarity to the drug in all ^{1}H assignments, except at δ 4.23. The difference of the latter was due to the downfield shift of $–CH_2$ at position 10, similar to DP-I, which indicated the presence of –NH. The same was confirmed even from 2D COSY LC–NMR spectrum, which showed correlation among all ^{1}H peaks of the proposed structure.

3.5.3. DP-III

The experimental mass (427.2300 Da) of this photolytic product was ~2 Da less than the drug. The only possible chemical formula that justified the nitrogen rule was $C_{25}H_{27}N_6O^+$ (427.2240 Da). The formula had two hydrogens less than the drug, suggesting presence of an additional double bond or ring formation in the structure. The on-line H/D exchange studies showed absence of any labile hydrogen. This indirectly indicated that the lone labile hydrogen in the drug, i.e., –NH of tetrazole (position 27, Fig. 4), was utilized in cyclization. Also, the MS/TOF fragments (*m*/*z* 399, 233, 205 and 178) of DP-III were 2 Da less than the corresponding fragments of the drug (*m*/*z* 401, 235, 207 and 180). Taking into consideration these facts, the fragmentation pathway for the photolytic degradation product was outlined, which is included in Fig. 6. The LC–^{1}H NMR data (Table 6) of DP-III showed seven distinct ^{1}H peaks in the aromatic region, instead of the six peaks for the drug. Moreover, the presence of a singlet at δ 8.39 indirectly indicated that the phenyl ring was meta and para substituted, so that only ortho hydrogen was not surrounded by any hydrogen of the neighbouring carbon. Further, *H*16 showed no correlation with other hydrogens in 2D COSY LC–NMR spectrum (Fig. 5). All this could only be justified if *N*1 of tetrazole was attached to the phenyl ring at meta position to form a cyclized product.

3.6. Mechanistic explanation to the origin of the degradation products

The mechanisms of formation of all three DPs (I–III) from the drug are given in Fig. 7. The formation of DP-I in acidic condition is explained by sequential hydrolysis of amide and imine groups of irbesartan [19–20]. DP-II is generated from the drug by simple amide hydrolysis in basic condition [19]. The exposure of drug to UV radiations results in promotion of π-electrons to a non-bonding orbital yielding two aryl radicals, one of which attacks the adjacent tetrazole ring to give cyclized DP-III in a photooxidation process [21].

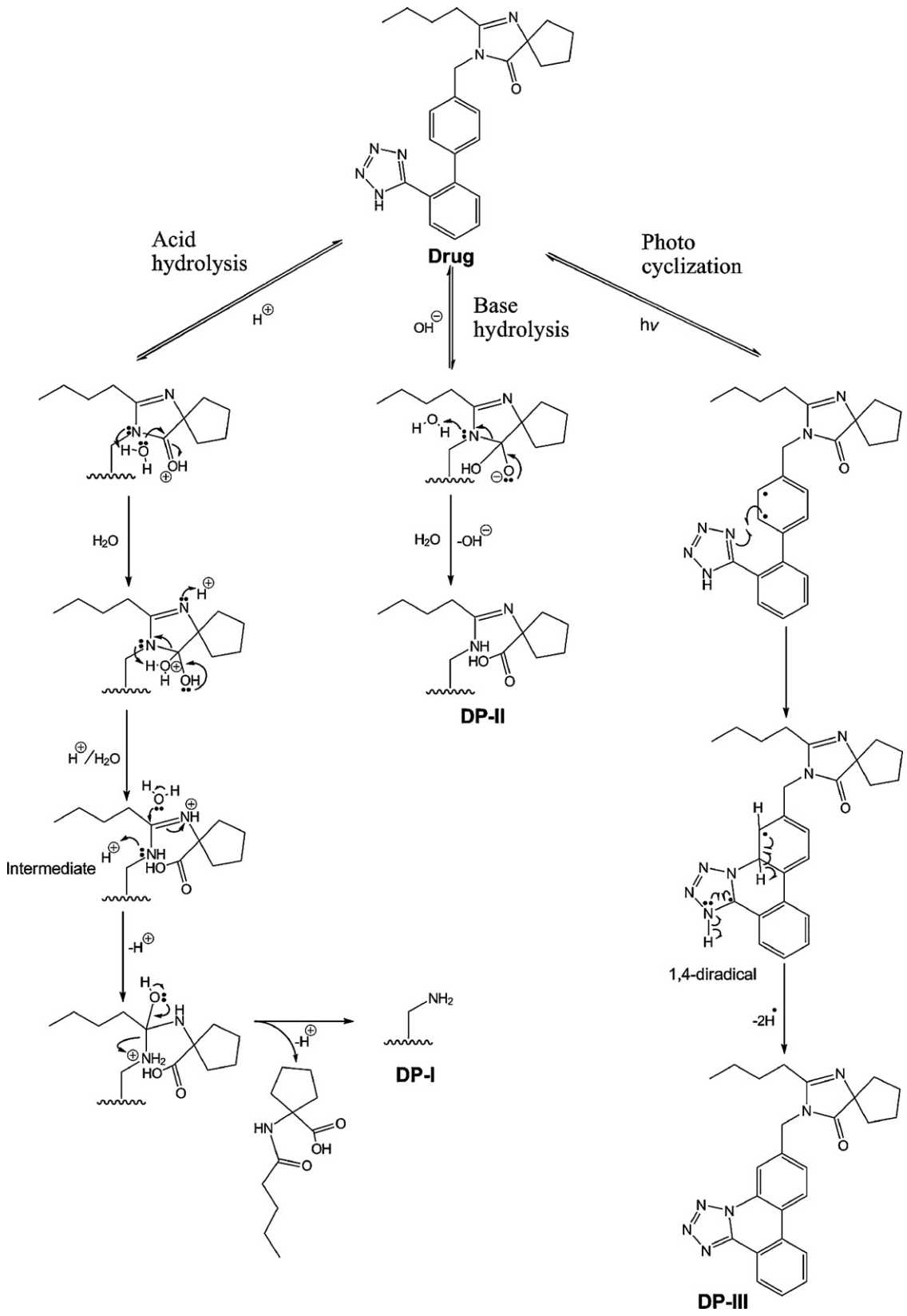

Fig. 7. Mechanism of formation of DPs from the drug.

4. Conclusion

Stress degradation studies on irbesartan, carried out according to ICH guidelines, provided information on the degradation behaviour of the drug under conditions of hydrolysis, oxidation, photolysis and thermal stress. HPLC analyses revealed formation of three degradation products (I–III), all of which were hitherto unknown. The degradation products were characterized with the

help of LC–MS TOF data, on-line H/D exchange, and ^{1}H and 2D LC–NMR studies. DP-I formed under acidic condition was characterized to be (2′-(1H-tetrazol-5-yl)biphenyl-4-yl)methanamine, whereas DP-II was identified as 1-(1-((2′-(1H-tetrazol-5-yl)biphenyl-4-yl)methylamino)pentylideneamino)cyclopentane carboxylic acid. The photolytic product (DP-III) was found to be a tetra cyclic compound, viz., 2-butyl-3-(tetrazolo[1,5-f]phenanthridin-6-ylmethyl)-1,3-diazaspiro[4.4]non-1-en-4-one. The structures were further justified by mechanisms of their formation.

References

[1] ICH, Stability testing of new drug substances and products Q1A(R2), in: International Conference on Harmonisation, IFPMA, Geneva, 2003.

[2] WHO, Draft Stability Testing of Active Pharmaceutical Ingredients and Pharmaceutical Products, World Health Organization, Geneva, 2007.

[3] CPMP, Note for Guidance on Stability Testing: Stability Testing of Existing Active Substances and Related Finished Products, Committee for Proprietary Medicinal Products, EMEA, London, 2002.

[4] TPD, Guidance for Industry Stability Testing of Existing Drug Substances and Products, Therapeutic Products Directorate, Health Canada, Ottawa, ON, 2003.

[5] M. Bakshi, S. Singh, Development of validated stability-indicating assay methods—critical review, J. Pharm. Biomed. Anal. 28 (2002) 1011–1040.

[6] S. Görög, The importance and the challenges of impurity profiling in modern pharmaceutical analysis, TrAC 25 (2006) 755–757.

[7] T. Murakami, T. Kawasaki, A. Takemura, N. Fukutsu, N. Kishi, F. Kusu, Identification of degradation products in loxoprofen sodium adhesive tapes by liquid chromatography–mass spectrometry and dynamic pressurized liquid extraction–solid-phase extraction coupled to liquid chromatography–nuclear magnetic resonance spectroscopy, J. Chromatogr. A 1208 (2008) 164–174.

[8] P. Novak, P. Tepes, M. Ilijas, I. Fistric, I. Bratos, A. Avdagic, Z. Hamersak, V.G. Markovic, M. Dumic, LC–NMR and LC–MS identification of an impurity in a novel antifungal drug icofungipen, J. Pharm. Biomed. Anal. 50 (2009) 68–72.

[9] T. Murakami, N. Fukutsu, J. Kondo, T. Kawasaki, Application of liquid chromatography-two-dimensional nuclear magnetic resonance spectroscopy using pre-concentration column trapping and liquid chromatography–mass spectrometry for the identification of degradation products in stressed commercial amlodipine maleate tablets, J. Chromatogr. A 1181 (2008) 67–76.

[10] R.V. Dev, G.S.U. Kiran, B.V. Subbaiah, B.S. Babu, J.M. Babu, P.K. Dubey, K. Vyas, Identification of degradation products in stressed tablets of rabeprazole sodium by HPLC-hyphenated techniques, Magn. Reson. Chem. 47 (2009) 443–448.

[11] R.P. Shah, V. Kumar, S. Singh, Liquid chromatography/mass spectrometric studies on atorvastatin and its stress degradation products, Rapid Commun. Mass Spectrom. 22 (2008) 613–622.

[12] J.R. Powell, R.A. Reeves, M.R. Marino, C. Cazaubon, D. Nisato, A review of the new angiotensin II-receptor antagonist irbesartan, Cardiovasc. Drug Rev. 16 (1998) 169–194.

[13] F.J. Morales-Olivas, I. Aristegui, L. Estan, J.L. Rodicio, A. Moreno, V. Gil, G. Ferrón, O. Velasco, The KARTAN study: a postmarketing assessment of irbesartan in patients with hypertension, Clin. Ther. 26 (2004) 232–244.

[14] C.J. Mbah, Kinetics of decomposition of irbesartan in aqueous solutions determined by high performance liquid chromatography, Pharmazie 59 (2004) 920–922.

[15] S. Hillaert, T.R.M. DeBeer, J.O. DeBeer, W.V. Bossche, Optimization and validation of a micellar electrokinetic chromatographic method for the analysis of several angiotensin-II-receptor antagonists, J. Chromatogr. A 984 (2003) 135–146.

[16] G. Wang, J.D. Fiske, S.P. Jennings, F.P. Tomasella, V.A. Palaniswamy, K.L. Ray, Identification and control of a degradation product in Avapro™ film-coated tablet: low dose formulation, Pharm. Dev. Technol. 13 (2008) 393–399.

[17] ICH, Stability testing: photostability testing of new drug substances and products Q1B, in: International Conference on Harmonisation, IFPMA, Geneva, 1996.

[18] R.A. Seburg, J.M. Ballard, T. Hwang, C.M. Sullivan, Photosensitized degradation of losartan potassium in an extemporaneous suspension formulation, J. Pharm. Biomed. Anal. 42 (2006) 411–422.

[19] J. March, Advanced Organic Chemistry, Reactions, Mechanisms and Structure, 4th ed., John Wiley and Sons, Singapore, 2005, pp. 384.

[20] J. March, Advanced Organic Chemistry, Reactions, Mechanisms and Structure, 4th ed., John Wiley and Sons, Singapore, 2005, pp. 885.

[21] D.E. Moore, in: H. Tonnesen (Ed.), The Photostability of Drugs and Drug Formulations, Taylor and Francis, London, 1996, p. 85.